Chemical Engineering Journal 463 (2023) 142431

Contents lists available at ScienceDirect

Chemical Engineering Journal

journal homepage: www.elsevier.com/locate/cej

Molecular mechanism of adsorbing triclocarban by the activated sludge in wastewater treatment systems

Hao Wang [a], Hanlin Cui [a], Xiaodan Ma [b], Carolyn R. Cornell [c], Liying Zhang [a], Yijun Ren [b], Minghan Li [a], Ying Liu [a], Shu-Hong Gao [b], Zhiling Li [a], Ai-Jie Wang [a,b], Jizhong Zhou [d,e], Bin Liang [b,*]

[a] State Key Laboratory of Urban Water Resource and Environment, School of Environment, Harbin Institute of Technology, Harbin 150090, China
[b] State Key Laboratory of Urban Water Resource and Environment, School of Civil & Environmental Engineering, Harbin Institute of Technology Shenzhen, Shenzhen 518055, China
[c] Department of Civil and Environmental Engineering, Rice University, Houston, TX 9 77005, USA
[d] Institute for Environmental Genomics and Department of Microbiology and Plant Biology, University of Oklahoma, Norman, OK 73019, USA
[e] School of Civil Engineering and Environmental Sciences, University of Oklahoma, Norman, OK 73019, USA

ARTICLE INFO

Keywords:
Triclocarban (TCC) adsorption
Extracellular polymeric substances (EPS)
Ammonia transporter
Molecular simulation
Activated sludge

ABSTRACT

The ubiquitous use of antimicrobial triclocarban (TCC) has raised widespread concern about the potential impacts on wastewater treatment systems, the environment, and the human population. As important constituents of activated sludge secretions, extracellular polymeric substances (EPS) play essential roles in removing micropollutants during wastewater treatment. Here, the adsorption of TCC by sludge and EPS in a multistage biological process was investigated. The EPS was enriched upon TCC stress, and the adsorption by sludge and EPS showed multilayer heterogeneity. The adsorption constant K_f (6.3794–7.6061) of EPS was over 10 times higher than that of sludge (0.5661–0.6200) in all stages, potentially owing to the loose multilayer structure and substantial functional groups (tryptophan-protein as the main binding site) in EPS. TCC significantly inhibited the biological removal of ammonia nitrogen. Notably, TCC once reaching the cell surface, formed a stable complex with ammonia transporter (Amt, binding energy: -73.1 ± 16.6 kJ·mol^{-1}) and bound to the selectivity filter vestibule of Amt (tryptophan 144 and serine 227), inhibiting the transport of ammonia. Our work drew molecular-level insights into the interaction between TCC and activated sludge, and evaluated the adverse impacts on treatment performance through an in silico approach, providing new information on the fate and risk of TCC in wastewater treatment systems.

1. Introduction

Triclocarban (TCC), a typical antimicrobial agent added to detergents, personal care products and textiles, has been widely detected in wastewater treatment systems and environmental media. The global annual use of TCC has exceeded 2000 tons with the annual use in China alone reaching 1220 tons [1,2]. The use of TCC has continued to grow with the increasing consumption of personal care products in the post-COVID-19 pandemic era [3]. Most TCC is collected by sewers and enters wastewater treatment plants (WWTPs), making WWTPs a main source of TCC in receiving waters [4]. Although WWTPs remove 97% of TCC from water, TCC is often present in activated sludge due to its recalcitrance to biodegradation [4]. A previous study reported that only 21% of TCC was metabolized whereas the majority of the remaining TCC was adsorbed into sludge during wastewater treatment [5]. Activated sludge determines the fate of TCC as it is where the interaction and adsorption of most TCC occurs. The mean accumulative concentrations of TCC have been shown to reach up to 39 and 8.45 mg·kg^{-1} in sewage

Abbreviations: TCC, triclocarban; EPS, extracellular polymeric substances; S-EPS, soluble extracellular polymeric substances; LB-EPS, loosely bound extracellular polymeric substances; TB-EPS, tightly bound extracellular polymeric substances; PN/PS, proteins/polysaccharides ratio; FTIR, Fourier transform infrared spectra; EEM, excitation emission matrix spectra; UPLC, ultra-performance liquid chromatography; WWTPs, wastewater treatment plants; HA-A/O, Hydrolytic acidification anaerobic-anoxic/oxic; Amt, ammonium transporter; RDSM, root mean square deviations; Rg, radius of gyration; MLSS, mixed liquor suspended solids.

* Corresponding author.
E-mail address: liangbin1214@hit.edu.cn (B. Liang).

https://doi.org/10.1016/j.cej.2023.142431
Received 6 January 2023; Received in revised form 27 February 2023; Accepted 10 March 2023
Available online 15 March 2023

sludge from the United States and China, respectively [6,7]. Due to this strong absorption of TCC to sludge, it can then be released into the environment along with residual sludge with the detection level of TCC in environmental sediments reaching mg·kg^{-1} level in several cases [5,8]. TCC may adversely affect aquatic organisms (e.g., beneficial algae) and can enter the human food chain, potentially posing risks to pregnant women by increasing the risk of fetal defects [5,9,10]. Therefore, exploring the adsorption behavior and mechanism of TCC in sludge is necessary for an in-depth understanding of the fate and risk of TCC during wastewater biological treatment.

Activated sludge processes have varying adsorption capabilities due to its distinct characteristics in different treatment processes [11-13]. The surface properties of sludge (the type of surface charge, functional groups, specific surface area, etc.) affect the adsorption performance of sludge, and pH and temperature may also matter. Researchers have found that the outer shell of activated sludge is composed of abundant extracellular polymeric substances (EPS) [11,14-16]. EPS produced by sludge microorganisms can provide numerous binding and adsorption sites for micropollutants owing to the hydrophobic groups (e.g., amino, carboxyl, hydroxyl, and phosphate bonds) from proteins, polysaccharides, and other cellular secretion and lysis products [17-20]. Therefore, the type and quantity of EPS have a significant impact on the adsorption of activated sludge. For example, sequence batch reactors sludge secretes more proteins and has better adsorption of ciprofloxacin than activated sludge [11]. Although sludge adsorption is known to be an important pathway for TCC migration, the interaction between TCC and EPS as well as the adsorption mechanisms remain poorly understood.

Most WWTPs use a combination of processes to remove carbon, nitrogen, and phosphorus from wastewater [21]. A hydrolytic acidification-anoxic/aerobic (HA-A/O) process integrates multiple techniques to improve the treatment of industrial and municipal wastewater [22]. The HA section achieves thorough microbial decomposition of organic pollutants [23], and the A/O process has the potential to simultaneously remove nitrogen and phosphorus, while also ensuring cost-effectiveness and efficiency [24]. The removal of ammonia nitrogen is crucial to ensuring that the effluent fulfills the quality level[25]. Toxic pollutants in sewage hinder ammonia nitrogen removal by inhibiting N-removal microorganisms, restricting the transport of ammonia, and hindering the transformation of ammonia nitrogen by N-removal microorganisms [26]. In our previous work, we discovered that TCC undergoes both adsorption and biodegradation throughout the HA-A/O process and inhibits ammonia nitrogen removal [27]. However, discrepancies were observed in the adsorption of TCC by the sludge from different treatment sections, and binding mechanisms remain unclear. As EPS is as an important and inseparable part of sludge, elucidating the role of EPS during the adsorption of TCC is necessary.

In order to fill these knowledge gaps, the adsorption behavior and mechanism of TCC in sludge in different operational sections (hydrolytic acidification, anoxic, and aerobic section) were investigated. The objectives of this study were to: (i) investigate the adsorption behavior of TCC in each section of HA-A/O and the affinity of different sludge; (ii) explore the role of EPS and the adsorption mechanism in the removal of TCC; and (iii) elucidate the binding of TCC to ammonia transport proteins (Amt) and the impact on ammonia nitrogen removal. Together, our findings provide in-depth insights into the intrinsic mechanisms of the adsorption of TCC in different sludge types, evaluate the impact on treatment performance, and expand the understanding of TCC migration as well as the adsorption pattern of broader emerging organic contaminants in biological processes.

2. Materials and methods

2.1. Standards and reagents

TCC (≥98%) was purchased from Aladdin (Shanghai, China). NaN_3, chromatographic grade methanol, and acetonitrile (>99.9%) were obtained from Sigma-Aldrich (USA). Unless otherwise stated, all other chemicals (>99.9%) were obtained from Kemiou Chemical Reagent Co. Ltd. (Tianjin, China).

2.2. Experimental device and operation

The HA-A/O reactor (Fig. S1) was operated in continuous flow for 80 days at different stages (details of the reactor working conditions in Supporting Information (SI)). The reactor was fed with synthetic wastewater. No TCC was introduced during the first 20 days to adapt the sludge (Stage i). The reactor was then operated for another 60 days at different influent TCC concentrations (Stage ii: 1 mg·L^{-1} TCC from days 21 to 40; Stage iii: 5 mg·L^{-1} TCC from days 41 to 60 and Stage iv: 8 mg·L^{-1} TCC from days 61 to 80).

2.3. TCC adsorption by inactivated AN, ANO, and O sludge

Three sections of sludge were taken from the HA-A/O reactor: anaerobic (AN), anoxic (ANO), and aerobic (O). TCC adsorption by AN, ANO, and O sludge was evaluated using a series of batch sorption tests. The sludge samples were taken on day 20 (0 mg·L^{-1} TCC) and washed three times with phosphate buffered saline (PBS, 0.01 mM). No background TCC was observed after washing. The sludge samples were then placed into a series of 50 mL brown conical flasks with a MLSS concentration of 2 g·L^{-1}. Sodium azide (NaN_3, 0.1% w/v) was added into each flask to inhibit possible degradation of TCC by the sludge [11]. During the experiments, each shake flask was a sampling point (each point with 2 replicates) with TCC in the aqueous phase. EPS and activated sludge were separated from the TCC in the aqueous phase using centrifugation at 5000 rpm for 15 min. Then, EPS was extracted using a thermal extraction method [28], and EPS (aqueous phase) and sludge were then separated by centrifugation (9000 rpm, 15 min). All samples were lyophilized (FD-1–50, BIOCOOL, China), redissolved in methanol, and filtered through a 0.45 μm organic membrane before being analyzed using Ultra-Performance Liquid Chromatography (UPLC, Waters, USA). The removal efficiency of TCC and specific adsorption (qt) were examined (SI). Langmuir (1) and Freundlich (2) adsorption isotherm models were applied to fit the experimental data (SI).

2.4. The binding experiments of TCC and EPS

The binding experiments were conducted at a range of TCC concentrations to examine the adsorption by EPS. On day 20, EPS (prepared as described in section 2.3) was separated from sludge samples of each section (AN, ANO, and O), purified using a 0.45 μm filter, and lyophilized. Deionized water was used to dissolve the lyophilized EPS, yielding a resolution of 20 mg·L^{-1} EPS. Then, various volumes of TCC mother liquor (30 g·L^{-1}) were mixed with the EPS solution. The TCC concentration range included: 50, 100, 500, 800, 1000, 3000, 5000, 8000, and 10000 μg·L^{-1} with two replicates. The pH of the EPS-TCC solutions was adjusted to 7.0 ± 0.2 using 0.1 M HCl/NaOH. The EPS-TCC sample tubes were placed in a 150 rpm light-proof shaker at 30 ± 0.1℃ and mixed for 4 h to reach adsorption equilibrium before spectral analysis.

2.5. Analytical methods

2.5.1. Chemical analysis

Polysaccharides and proteins were determined by the phenol sulfate method [29] and Micro BCA protein assay kit (Sangon Biotech, China). The contents of TCC were analyzed by UPLC (Waters, USA) with a reverse phase C18 column (Waters, USA) in gradient elution mode at a flow rate of 0.10 mL min^{-1} at 275 nm [27].

2.5.2. Spectral analyses

In order to reveal the mechanism of EPS binding to TCC

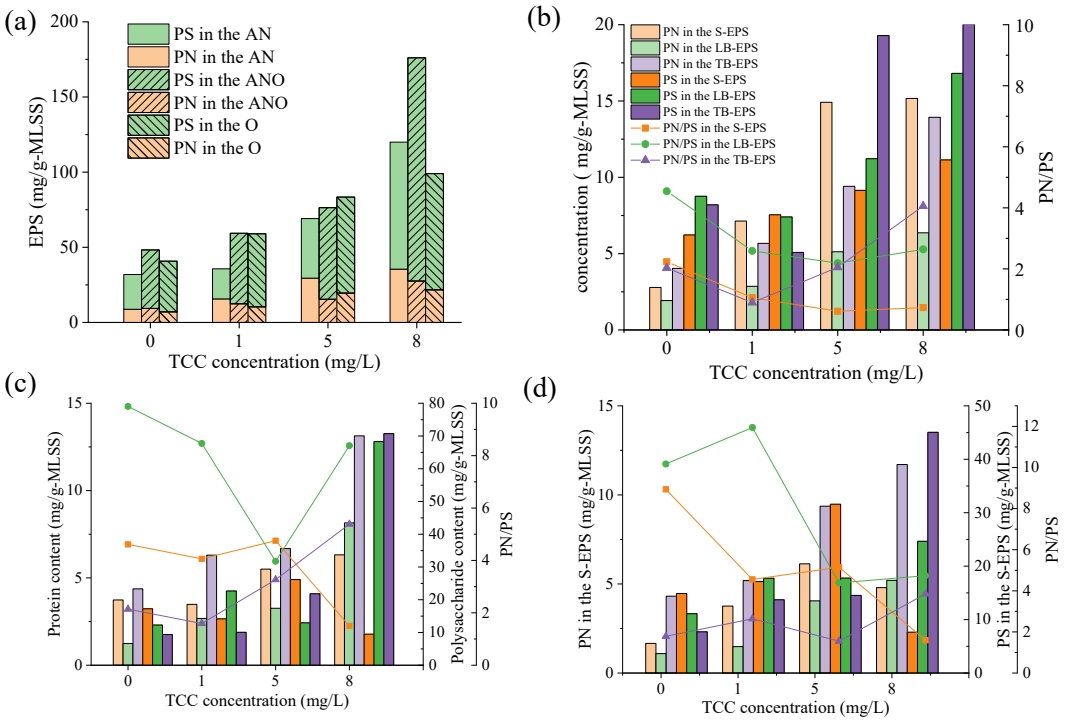

Fig. 1. Compositions of EPS in the AN, ANO and O sections from the HA-A/O process. Total concentration of EPS (a); PN, PS and PN/PS ratio of EPS from the sludge in AN (b), ANO (c) and O (d) section, respectively.

(fluorescence quenching technique) and the effect of TCC on the EPS content in AN, ANO, and O sections of sludge, a three-dimensional excitation-emission matrix (3D-EEM) fluorescence scan was performed by a fluorescence spectrophotometer (JASCO FP-6500, Japan). The wavelengths of excitation (E_x) and emission (E_m) were scanned from 250 to 500 nm and 250 to 550 nm, respectively, with a scanning interval of 5 nm and a sensitivity of 700 V.

Fourier transform infrared (FTIR) spectroscopy (Spectrum One B, PerkinElmer, USA) was performed to determine the functional groups responsible for binding TCC in the EPS extracted from AN, ANO, and O section sludge samples. The lyophilized EPS powder was mixed and ground with KBr at a mass ratio of 1:100, and pressed into thin slices for FTIR.

2.5.3. Molecular docking and molecular dynamics simulation

In order to explore the impact and molecular mechanism of TCC on ammonia transport, the transmembrane ammonia transporter protein (Amt) PDB ID: 6eu6 was chosen, and the gene sequence shared high homology with two genes (72.2% and 75.6% homology) in the AN sludge metagenomic (Table S2). Molecular docking of TCC and Amt protein, molecular dynamics, and binding energy-related calculations were done separately using the Yinfu cloud platform (https://cloud.yinfotek.com). The following parameters were set: molecular docking box centers (-12.572, −38.25, 16.508) and box sizes (36.566, 31.436, 29.152). Kinetic parameters were as follows: pressure of 1 atm and non-bond truncation value of 10 Å (SI for the more detailed relevant parameters).

2.5.4. Statistical analyses

One-way analysis of variance (ANOVA) was used to assess differences in sludge secretion EPS under different TCC concentration conditions performed by SPSS 16.0. Adsorption kinetics simulations were performed using the statistical functions of Origin 2018b. Parallel factor (PARAFAC) analysis was performed in Octave 7.10. For fluorescence EEM spectra, PARAFAC models with 2 to 5 components were calculated, and the correct three components were identified by analysis of residuals, split-edge tests, and database comparisons (results are uploaded at: https://openfluor.lablicate.com/of/measurement/9066).

3. Results and discussion

3.1. Characterization of the EPS in HA-A/O process at different TCC concentrations

The concentration and composition of EPS were investigated at 0, 1, 5, and 8 mg·L^{-1} TCC consecutive stress. The concentration of EPS in sludge samples increased significantly with increasing TCC concentration in AN (31.9, 35.7, 69.1, and 119.9 mg·gMLSS^{-1}, $p < 0.05$), ANO (48.2, 59.3, 76.3, and 176.1 mg·gMLSS^{-1}, $p < 0.05$) and O (40.8, 59.0, 83.4, and 99.0 mg·gMLSS^{-1}, $p < 0.05$) (Fig. 1a). The increase in TCC concentrations stimulated the generation of EPS in all sections. This observation is consistent with a previous study in which increasing TCC concentration (0 to 20 mg·L^{-1}) enhanced loosely bound-EPS (LB-EPS) and tightly bound-EPS (TB-EPS) contents from 20.95 to 31.72 and from 53.98 to 68.02 mg TOC g·VSS^{-1}, respectively [30]. Increases in EPS can help defend against toxic substances and harsh external environments [31] such as those experienced with increasing TCC concentrations.

The EPS extracted from AN, ANO, and O sludge samples had nearly identical compositions, with protein (PN) and polysaccharide (PS) being the predominant components (Fig. 1a). For all sludge types, both PN and PS contents increased with increasing TCC concentration (Fig. 1b-d). The PN portion of EPS can interact with contaminants and reduce the toxic effects of antimicrobial agents on microorganisms [11,32]. Moreover, the PN/PS mass ratio is frequently used to evaluate the hydrophobicity of sludge and accessibility to adsorption positions [11]. The increase in the influent TCC concentration resulted in a constant decrease in the PN/PS of soluble-EPS (S-EPS) in the three different sludges. The PN/PS of LB-EPS decreased at 0–5 mg·L^{-1} TCC (PN/PS in AN, ANO, and O sections decreased from 4.45 to 2.18, 9.98, to 3.96 and 10.17 to 4.38, respectively) before an increase at 8 mg·L^{-1} (PN/PS raised to 2.41, 8.38, and 4.73, respectively) in the three sections. The overall trend of PN/PS of TB-EPS was increased at 0–8 mg·L^{-1} TCC in

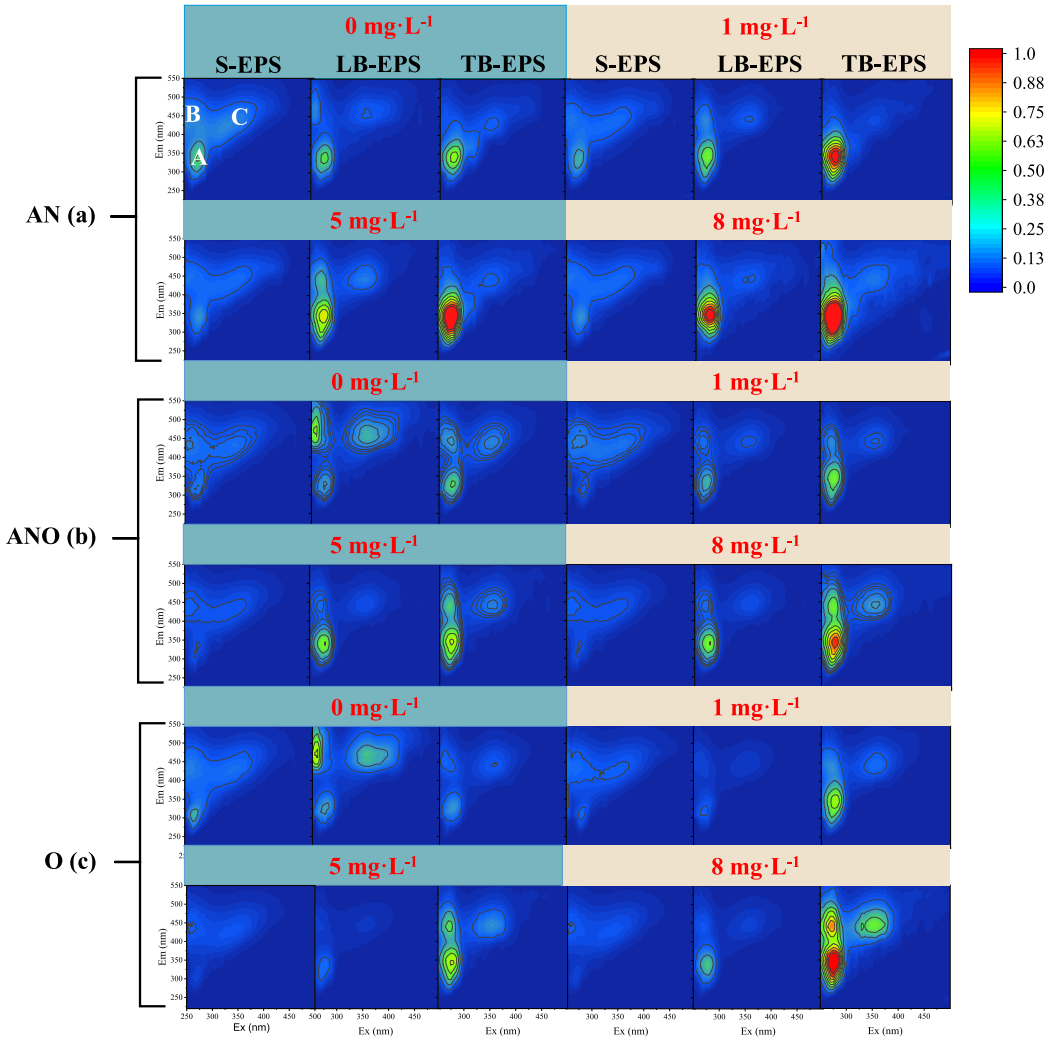

Fig. 2. EEM fluorescence spectra (normalized) of S-EPS, LB-EPS and TB-EPS in the AN (a), ANO (b) and O (c) section with the concentration of TCC 0, 1, 5 and 8 mg·L^{-1}, respectively.

the three sections (Fig. 1b-d). This implies that the stability of the sludge in the three sections decreased with increasing TCC concentration while forming richer aggregates [15]. In the AN and ANO sections, TB-EPS (47%-58%) was the dominant EPS subfraction while S-EPS (8.9%-21%) and LB-EPS (19%-43%) account for minor proportions at 8 mg·L^{-1} TCC. The content of PS and PN were generally higher in TB-EPS than that in LB-EPS after four operational stages under different TCC stress (Fig. 1cd). The EPS content in TB-EPS promoted formation of biofilms [33]. Comparable percentages of S-EPS (19%-45%) and TB-EPS (29%-57%) were found in the O section sludge, which indicated sufficient oxygen was present, and in turn, both the metabolic capability of microorganisms and the secretion of EPS were stimulated. This suggests that the sludge secretes more EPS and richer aggregates to counteract the toxic stress from TCC.

The fluorescence composition of the sludge EPS at different TCC concentrations was investigated. Based on EEM, three distinct fluorescence peaks were detected in all sludge EPS samples (Fig. 2). These peaks were found at 270–280/320–340 nm (peak A, tryptophan-like protein), Ex/Em: 260–280/420–450 (peak B, humic xanthic acid) and Ex/Em: 350–370/430–450 nm (peak C, hydrophobic humic acid) [34]. The fluorescence intensity noticeably increased as the influent TCC concentration increased. The increase in peak A (tryptophan-like protein) fluorescence intensity suggested that the prolonged exposure to TCC provoked the secretion of protein, which was consistent with the observed composition of EPS (Fig. 1b-d). Similar results have been previously observed in which both protein and polysaccharide contents of EPS in four different sludge (primary sludge, thickened sludge, dewatered sludge, and anaerobic digested sludge) were enriched with increasing triclosan concentration [35]. Furthermore, the fluorescence signal of tryptophan-like proteins in all sludge samples was significantly enhanced with increasing TCC concentration, suggesting their crucial role in the adsorption of TCC by EPS.

3.2. Adsorption of TCC by AN, ANO, and O sludge

The removal of TCC can reach 78–92% during adsorption and biological processes [5] for which EPS potentially provides a large number of active sites [11,36]. A sequencing batch adsorption experiment was performed to explore the role of EPS in the adsorption of TCC, employing the EPS extracted from sludge in each section. The results indicated that adsorption was the primary removal mechanism for TCC within 24 h. Specifically, up to 15.7 ± 0.5%, 14.5 ± 0.3%, and 13.6 ± 0.3% of TCC were adsorbed by EPS from the AN, ANO, and O sludge, respectively. The similar removal efficiencies might attribute to the similar amount of EPS secreted by the sludge in all three sections. The adsorption of TCC to each sludge EPS during the experimental period was shown in Fig. 3a-c. During the first five minutes, TCC was rapidly adsorbed to EPS, and similar adsorption patterns were observed for samples from all sludge sections ($p > 0.05$). However, the adsorption of TCC remained relatively stable from 0.05 to 24 h, possibly due to the

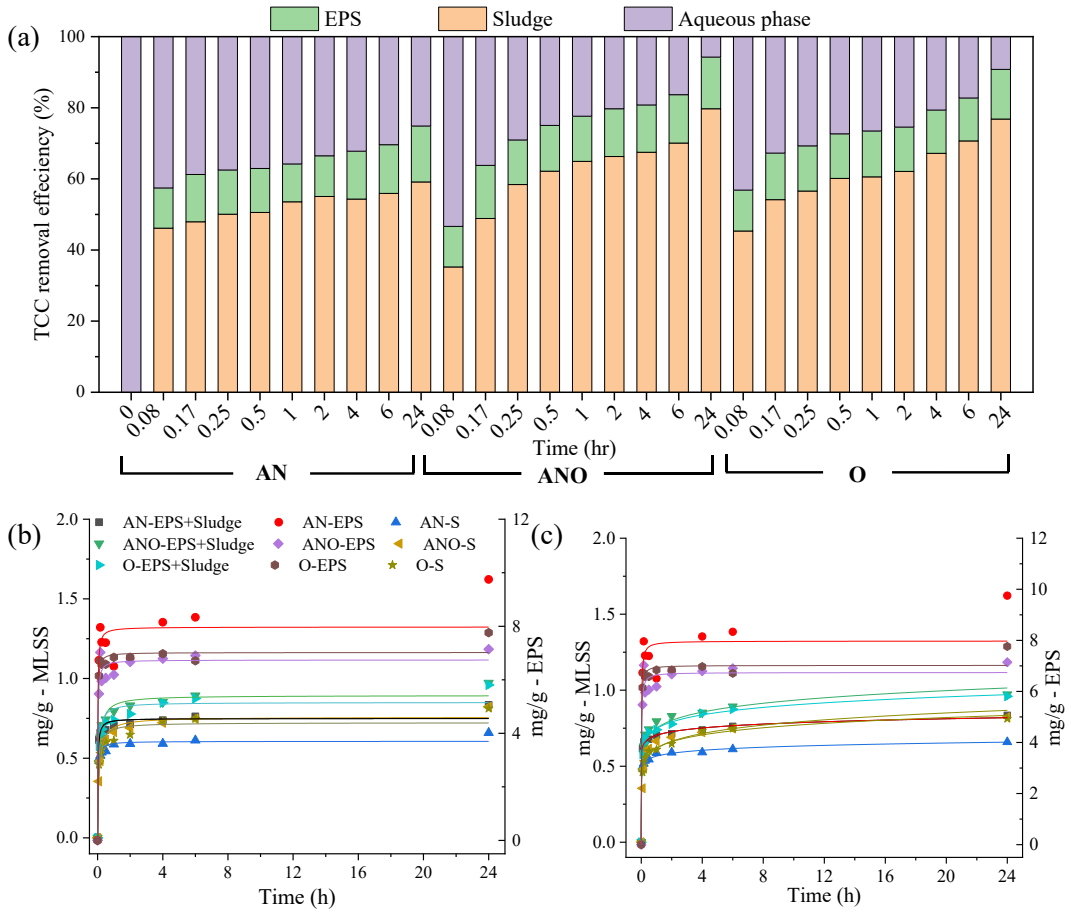

Fig. 3. Adsorption of TCC by AN, ANO, and O sludge. The initial TCC concentration was 2 mg·L^{-1}. TCC removal efficiency by Sludge, EPS, and Sludge + EPS of AN, ANO, and O sludge (a). Langmuir (b) and Freundlich (c) adsorption isotherm fit of TCC adsorption by Sludge, EPS, and Sludge + EPS in AN, ANO, and O sludge, respectively. Axes in (b) and (c): mg·g-MLSS^{-1} means the adsorption of TCC on sludge and sludge + EPS; mg·g^{-1} means the adsorption of TCC on EPS.

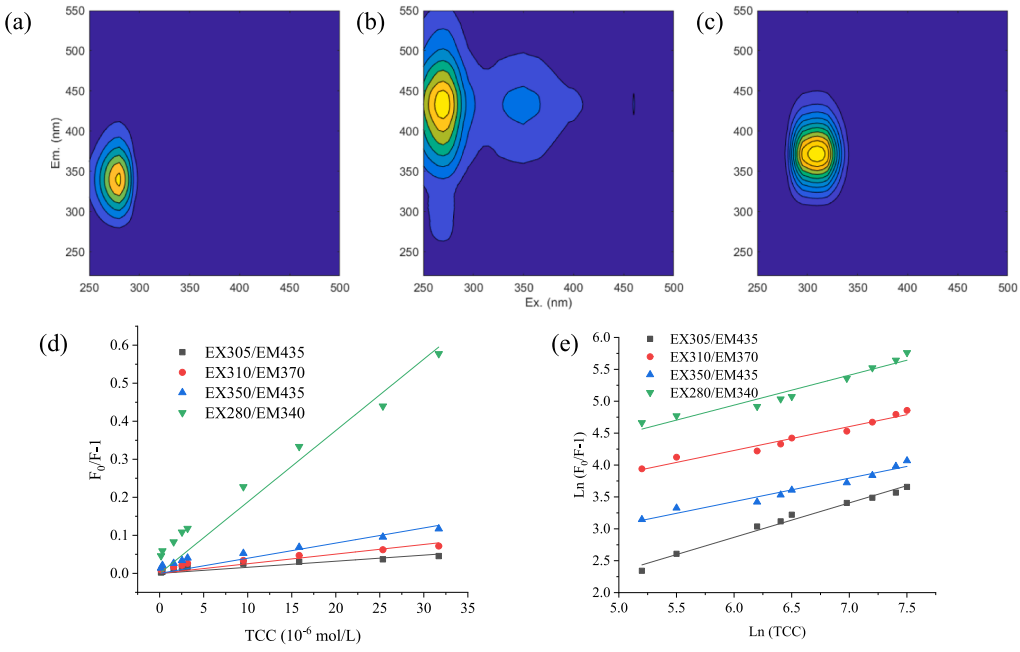

Fig. 4. The EEM spectrum of EPS decomposed by PARAFAC and the tryptophan-like protein (a), hydrophobic humic acid, (b) and xanthic acid (c). Fitting results for fluorescence intensities of components of tryptophan-like protein (EX280/EM340), hydrophobic humic acid (EX270/EM450; EX360/EM450) and xanthic acid (EX330/EM410) in EPS from AN, ANO, and O sludge with different TCC concentration using Sterne Volmer-equation(F_0/(F-1) and TCC concentrations) (d) and double-logarithm regression equation (e).

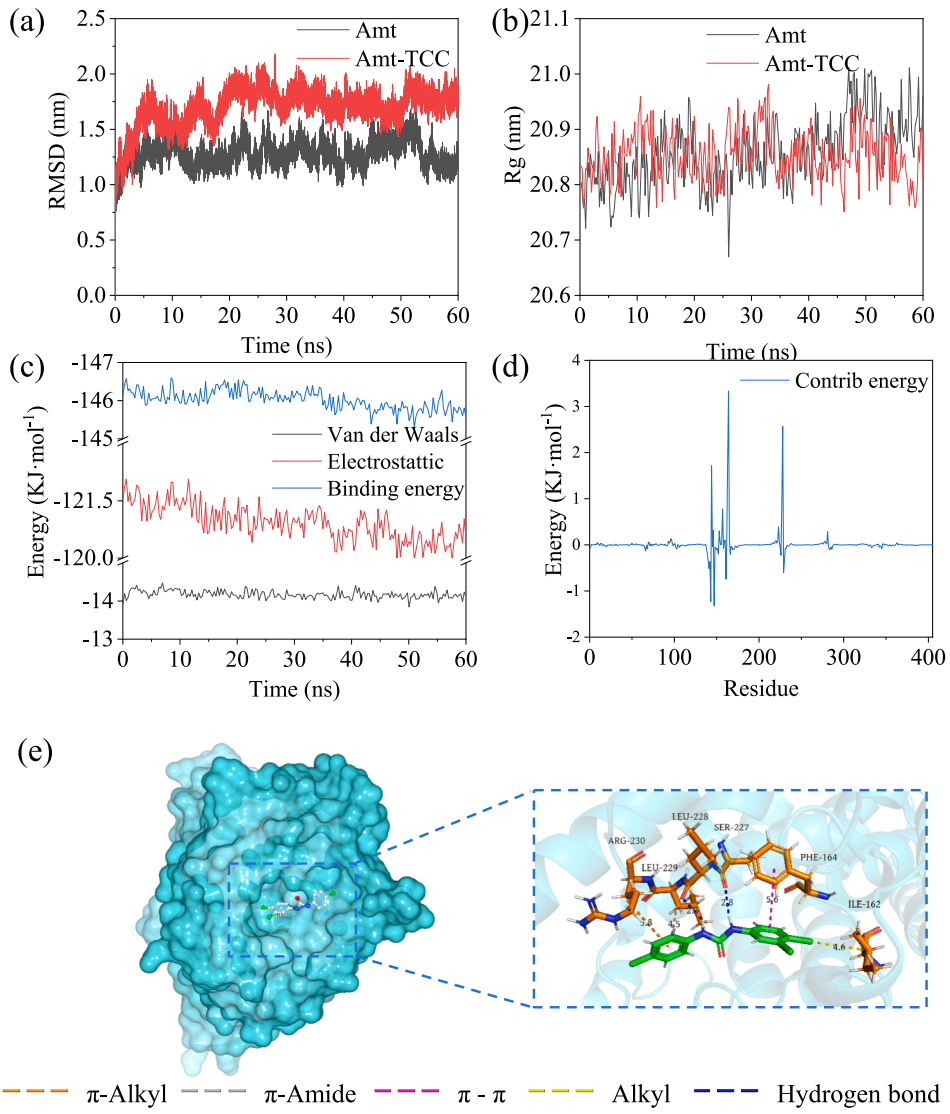

Fig. 5. Molecular dynamic (MD) simulation analysis of the binding process of the Amt (PDB ID:6eu6) structure with TCC: Comparison between the variation of root-mean-square-deviations (RMSD) (a), and radius of gyration (Rg) of Amt and Amt-TCC complex(b); The different types of binding energies (c), and the contribution of the ammonia residue (d), of Amt-TCC complex; The binding conformation of the Amt-TCC complex (e).

depletion of TCC at the adsorption positions.

The Freundlich and Langmuir isotherms (Fig. 3c) were used to describe the adsorption behavior of TCC by sludge, EPS, and the combination of sludge + EPS in the sequencing batch experiment (Table S1). The adsorption of TCC by sludge + EPS in all three sections agreed well with the Freundlich isotherm ($R^2 > 0.9661$), which indicated a sophisticated homogeneous process owing to a heterogeneous EPS structure over the whole adsorption site [11,30]. Moreover, the adsorption of TCC by EPS alone matched the Freundlich isotherm model ($R^2 > 0.9320$), indicating a multilayer biosorption pattern of TCC by the heterogeneous surfaces of EPS [28,34]. Similarly, The adsorption of TCC by denitrifying sludge fitted the Freundlich isotherm with a K_f value of 0.458 at 100 to 4000 μg·L^{-1} TCC was observed [37,38]. The energy binding constant K_f in the Freundlich model reflects the affinity of the adsorbent to bind to TCC, and the K_f values (binding energy constant) of TCC adsorption by EPS (7.6061, 6.3794, and 6.6760 for AN, ANO, and O section, respectively) were significantly greater than those by sludge (0.5661, 0.6163, and 0.6200, respectively) and sludge + EPS (0.7030, 0.7503, and 0.5664, respectively). These observations together suggested that EPS exhibited higher adsorptive affinity than sludge alone and sludge + EPS in the case of TCC adsorption. Within EPS, the highest K_f value of AN sludge EPS further suggested the highest affinity of the AN section as compared with the ANO and O sections. The adsorption kinetics showed that EPS binds to TCC by a multilayer heterogeneous structure with a K_f value one order of magnitude higher than that of the sludge. This suggests that EPS plays a very important role in the adsorption of TCC by sludge, providing a large number of adsorption sites with a small mass proportion.

3.3. Interaction between EPS and TCC

The content of EPS secreted by sludge in the three stages differed, but they had the same composition. EEM fluorescence quenching coupled with PARAFAC analysis was used to investigate the interaction between EPS and TCC as well as the intrinsic structural and conformational modifications of the fluorescent groups in EPS. As a type of interaction between EPS and TCC, quenching involves static and dynamic processes and can be examined by the Stern-Volmer equation. Specifically, static quenching is caused by the development of a non-fluorescent complex between the fluorophore and the quencher; whereas dynamic quenching is caused by a collision between the excited fluorophore and the quencher [36]. The extracted EPS was mainly composed of a

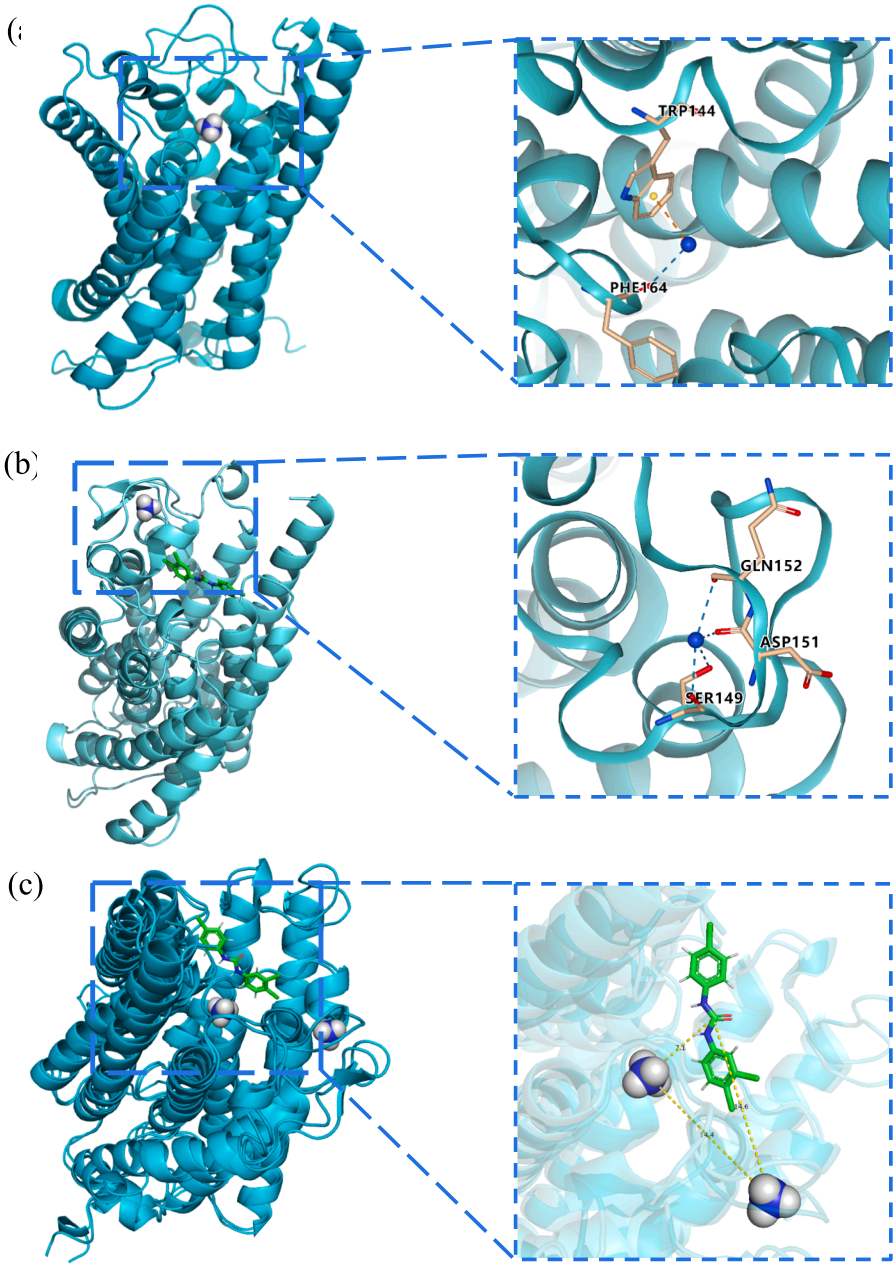

Fig. 6. The docking conformation of Amt domain and NH_4^+ (a), Amt domain-TCC and NH_4^+ (b) and assign of the two structures (c).

tryptophan-like (C1, 280/340, Fig. 4a) substance, a hydrophobic humic acid (C2, 270/450; 360/450, Fig. 4b), and a xanthic acid (C3, 330/410) based on the PARAFAC analysis (Fig. 4c and Table S4) [39].

The linear regression of the PARAFAC analysis of the fluorescence quenching data calculated K_q values of 5.32×10^{15} ($R^2 = 0.9725$), 3.25×10^{16} ($R^2 = 0.9154$), and 2.5×10^{16} ($R^2 = 0.9219$) $L{\cdot}mol^{-1}{\cdot}s^{-1}$ for tryptophan-like proteins, hydrophobic humic substances, and xanthates (Fig. 4), respectively. All values were magnitudes larger than the maximum diffusive collisional quenching rate constant of 2.0×10^{10} $L{\cdot}mol^{-1}{\cdot}s^{-1}$ for various bursting agents with biomolecules [40]. Therefore, the quenching of fluorescence intensity may be owed to the formation of EPS-TCC complexes instead of dynamic collision.

For binding involving a static burst mechanism, the modified double logarithmic equation can be used to determine the apparent binding constants and the number of binding positions, assuming the presence of independent binding positions in EPS [41]. To further determine the binding permanent (K_b) and the number of binding positions (n) on EPS during the static quenching, a double logarithmic regression equation was employed to fit the experimental data (all with $R^2 > 0.90$) [41]. As shown in Fig. 4, for tryptophan protein, hydrophobic humic acid and xanthic acid, the n values were 0.47, 0.54, 0.37, and 0.37, while the binding constants were 1.33×10^2 ($R^2 = 0.9472$), 0.42 ($R^2 = 0.9842$), and 16.71 ($R^2 = 0.9602$) $L{\cdot}mol^{-1}$, respectively (Fig. 4d). The binding strength of TCC to proteins was 1–3 orders of magnitude higher than the that to humic substances in EPS. Therefore, proteins may dominate the interaction between EPS and TCC.

3.4. Functional groups in binding TCC onto EPS

EPS is an important component of the sludge floc; in particular, the inner layer of TB-EPS directly contacts with the cell membrane. The exact functional groups involved in the binding of TCC to EPS in the three sludge sections were identified based on the FTIR analysis. The FTIR curves present the typical spectral bands of polysaccharides and

proteins (Fig. S2). The peak at 1661 cm^{-1} was associated with the stretching vibration of amide I (C = O) and the bending vibration of N-H [42,43]. Previous studies reported that the interaction between pollutants and proteins in EPS can result in a decreased amide bond absorption peak [14,36], and a red or blue shift [26,35]. The binding of TCC to EPS resulted in a red shift of the amide bonds of the sludge in all sludge samples further suggesting that proteins in EPS were involved in TCC adsorption. Interestingly, absorption peaks of S-EPS and LB-EPS were smaller at 1661 cm^{-1} and greater for TB-EPS. The interaction between TCC and the protein in EPS potentially reduced the absorption peak of the amide bond, while TB-EPS, through absorbing the amide bond introduced by TCC, expanded the absorption peak (SI for the molecular structure of TCC). Similarly, a previous study reported that the amide bond absorption peak of denitrifying sludge increased when the EPS was bound to TCC [37]. The TB-EPS of all sludge showed a significant blue shift in the P-O stretching vibration at 1071 cm^{-1}, which suggested that TCC would bind to organophosphorus functional groups [44]. In addition, a red shift of the O = C–O (corresponding to carboxylate groups) at 1453 cm^{-1} was observed for the TB-EPS-TCC of AN, ANO, and O sludge samples [45]. In particular, the 995–1090 cm^{-1} region was assigned to C-H stretching vibrations [46], and the TCC-EPS in the three sections showed a red shift, indicating that polysaccharides may also be another site for TCC adsorption.

3.5. Molecular insight into the binding property of EPS and TCC

TCC continuously migrates to the sludge microbial cell surface via EPS and inevitably contacts and affects cell membrane proteins. Several studies have shown that TCC (1 $mg{\cdot}L^{-1}$) affects ammonia nitrogen removal in HA-A/O reactors and nitrification reactors [27,30]. The effect of TCC on ammonia transport proteins (Amt), which are important NH_4^+ transport channels, was investigated by using molecular docking and molecular dynamics simulations [47]. The RMSD of the molecular trajectory during the binding of the Amt structural domain to TCC was stable after 30 ns (Fig. 5a). The TCC-Amt binding underwent conformational fluctuations and gradually formed a stable structure. In particular, the Rg (representing the compactness of the protein [48]) of TCC-Amt slightly decreased (Fig. 5b), indicating that the TCC resulted in a more compact Amt protein structure possibly affecting the NH_4^+ binding and transport. The Amt domain was bound to TCC mainly by electrostatic force and supplemented by van der Waals force (Fig. 5c). Furthermore, molecular dynamic simulations revealed that the minimum binding energy of TCC to Amt was -73.1 ± 16.6 $kJ{\cdot}mol^{-1}$, which was much lower than the known minimum binding energy of sulfamethoxazole (-31.73 $kJ{\cdot}mol^{-1}$) and phenol (-19.51 $kJ{\cdot}mol^{-1}$) [26,49]. These observations implied that TCC was more easily bonded to Amt than sulfamethoxazole and phenol, resulting in a stable structure. The lower binding energy and more stable binding structure could cause a stronger reduction of Amt activity by TCC as compared with sulfamethoxazole and phenol. This might imply a stronger impact of TCC on functional species than sulfamethoxazole and phenol, which requires further studies.

Amino acid residues with absolute binding free energy values>0.5 $kJ{\cdot}mol^{-1}$ were chosen to investigate the contributions of the amino acids of the Amt domain to TCC binding (free energy, Fig. 5d, Table S4). Residues aspartic acid (ASP)163 (1.88 $kJ{\cdot}mol^{-1}$), tryptophan (TRP) 144 (1.72 $kJ{\cdot}mol^{-1}$), serine (SER) 227 (0.97 $kJ{\cdot}mol^{-1}$), lysine (LYS) 157 (0.78 $kJ{\cdot}mol^{-1}$), leucine (LEU) 147 (-1.32 $kJ{\cdot}mol^{-1}$), alanine (ALA) 143 (-1.23 $kJ{\cdot}mol^{-1}$), phenylalanine (PHE) 161 (-0.75 $kJ{\cdot}mol^{-1}$), LEU229 (-0.60 $kJ{\cdot}mol^{-1}$), and histidine-E type (HIE) 141 (-0.51 $kJ{\cdot}mol^{-1}$) played important roles in the binding of Amt to TCC. Among them, residues PHE164 (bond distance 5.4 Å), SER227 (2.8 Å), LEU228 (2.3 Å), and LEU229 (4.5 Å) bound to TCC near the docking pocket via Pi-Pi, hydrogen bonds, hydrogen bonds, and Amide-PI interactions, respectively (Fig. 5ef).

To investigate the effect of TCC on the binding of Amt to NH_4^+, the kinetically stabilized Amt-TCC structure was molecularly docked with NH_4^+. NH_4^+ can interact with Amt via the π-cation interaction of Trp144 and the hydrogen bond of PHE164. The residues SER149, ASP 151, and glutamine (GLN) 152 of TCC-Amt interacted with NH_4^+ through hydrogen bonding (Fig. 6); moreover, TCC squeezed the position of NH_4^+ (Fig. 6b), thus impacting the binding to NH_4^+. Importantly, both TRP144 and SER227 are selectivity filter vestibules of the Amt domain, and the occupancy of the binding site by TCC may interfere with NH_4^+ transport in microbial metabolism.

4. Conclusions

In this study, we elucidated the mechanisms of TCC adsorption by the EPS of sludge from three sections in the HA-A/O treatment process. Activated sludge bacteria can resist TCC toxicity by secreting EPS, especially polysaccharides and proteins. Adsorption kinetics revealed rapid adsorption of TCC at 5 min, and 30–50 $mg{\cdot}gMLSS^{-1}$ EPS contributed to 13%-16% of the adsorption (while sludge provided 59.1%-79.7%). The binding capacity of EPS was 10 times higher than that of sludge, potentially due to the static quenching of tryptophan-like proteins to TCC and various functional groups such as hydroxyl groups. Once reaching saturated adsorption, TCC migrates to the cell surface and binds to the ammonia transporter Amt, which robs the NH_4^+ binding pocket and selectivity filter vestibule, inhibiting NH_4^+ binding and transport. The results broaden the understanding of the adsorption of TCC by sludge and elucidating the role of EPS in TCC removal, hence clarifying the adverse impact of TCC on wastewater treatment systems.

Declaration of Competing Interest

The authors declare that they have no known competing financial interests or personal relationships that could have appeared to influence the work reported in this paper.

Data availability

Data will be made available on request.

Acknowledgements

The study was financially supported by the National Natural Science Foundation of China (Nos. 52293443, 52230004 and 42207147), the Guangdong Basic and Applied Basic Research Foundation (No. 2023B1515020077), Shenzhen Overseas High-level Talents Research Startup Program (No. 20210308346C), and Shenzhen Science and Technology Program (No. KQTD20190929172630447).

Appendix A. Supplementary data

Supplementary data to this article can be found online at https://doi.org/10.1016/j.cej.2023.142431.

References

[1] M.-J. Chen, Y.-T. Liu, C.-W. Lin, V.K. Ponnusamy, J.-F. Jen, Rapid determination of triclosan in personal care products using new in-tube based ultrasound-assisted salt-induced liquid–liquid microextraction coupled with high performance liquid chromatography-ultraviolet detection, Anal. Chim. Acta 767 (2013) 81–87.
[2] Z.-F. Chen, H.-B. Wen, X. Dai, S.-C. Yan, H. Zhang, Y.-Y. Chen, Z. Du, G. Liu, Z. Cai, Contamination and risk profiles of triclosan and triclocarban in sediments from a less urbanized region in China, J. Hazard. Mater. 357 (2018) 376–383.
[3] S. Adhikari, R. Kumar, E.M. Driver, T.D. Perleberg, A. Yanez, B. Johnston, R. U. Halden, Mass trends of parabens, triclocarban and triclosan in Arizona wastewater collected after the 2017 FDA ban on antimicrobials and during the COVID-19 pandemic, Water Res. 222 (2022), 118894.
[4] R.U. Halden, D.H. Paull, Co-occurrence of triclocarban and triclosan in US water resources, Environ. Sci. Tech. 39 (6) (2005) 1420–1426.
[5] H. Yun, B. Liang, D. Kong, X. Li, A. Wang, Fate, risk and removal of triclocarban: A critical review, J. Hazard. Mater. 387 (2020) 121944.

[6] R.U. Halden, On the Need and Speed of Regulating Triclosan and Triclocarban in the United States, Environ. Sci. Tech. 48 (7) (2014) 3603–3611.
[7] J. Chen, X.-Z. Meng, A. Bergman, R.U. Halden, Nationwide reconnaissance of five parabens, triclosan, triclocarban and its transformation products in sewage sludge from China, J. Hazard. Mater. 365 (2019) 502–510.
[8] F.-J. Peng, C.-G. Pan, M. Zhang, N.-S. Zhang, R. Windfeld, D. Salvito, H. Selck, P. J. Van den Brink, G.-G. Ying, Occurrence and ecological risk assessment of emerging organic chemicals in urban rivers: Guangzhou as a case study in China, Sci. Total Environ. 589 (2017) 46–55.
[9] J.R. Rochester, A.L. Bolden, K.E. Pelch, C.F. Kwiatkowski, Potential Developmental and Reproductive Impacts of Triclocarban: A Scoping Review, J Toxicol-Us 2017 (2017) 9679738.
[10] L. Wei, P. Qiao, Y. Shi, Y. Ruan, J. Yin, Q. Wu, B. Shao, Triclosan/triclocarban levels in maternal and umbilical blood samples and their association with fetal malformation, Clin. Chim. Acta 466 (2017) 133–137.
[11] H. Zhang, Y. Jia, S.K. Khanal, H. Lu, H. Fang, Q. Zhao, Understanding the Role of Extracellular Polymeric Substances on Ciprofloxacin Adsorption in Aerobic Sludge, Anaerobic Sludge, and Sulfate-Reducing Bacteria Sludge Systems, Environ. Sci. Tech. 52 (11) (2018) 6476–6486.
[12] M.N. Kinyua, M. Elliott, B. Wett, S. Murthy, K. Chandran, C.B. Bott, The role of extracellular polymeric substances on carbon capture in a high rate activated sludge A-stage system, Chem. Eng. J. 322 (2017) 428–434.
[13] Q. Wang, Q. Shen, J. Wang, J. Zhao, Z. Zhang, Z. Lei, T. Yuan, K. Shimizu, Y. Liu, D.-J. Lee, Insight into the rapid biogranulation for suspended single-cell microalgae harvesting in wastewater treatment systems: Focus on the role of extracellular polymeric substances, Chem. Eng. J. 430 (2022), 132631.
[14] Z. Li, C. Wan, X. Liu, L. Wang, D.-J. Lee, Understanding of the mechanism of extracellular polymeric substances of aerobic granular sludge against tetracycline from the perspective of fluorescence properties, Sci. Total Environ. 756 (2021), 144054.
[15] Z. Hou, X. Zhou, W. Dong, H. Wang, H. Liu, Z. Zeng, J. Xie, Insight into correlation of advanced nitrogen removal with extracellular polymeric substances characterization in a step-feed three-stage integrated anoxic/oxic biofilter system, Sci. Total Environ. 806 (2022), 151418.
[16] G.-F. Li, Z.-Q. Ren, Y. Wang, J.-P. Li, W.-J. Ma, Y.-F. Cheng, B.-C. Huang, R.-C. Jin, Molecular spectroscopy and docking simulation revealed the binding mechanism of phenol onto anammox sludge extracellular polymeric substances, Sci. Total Environ. 830 (2022), 154733.
[17] R. Späth, H.C. Flemming, S. Wuertz, Sorption properties of biofilms, Water Sci. Technol. 37 (1998) 207–210.
[18] G.-P. Sheng, H.-Q. Yu, X.-Y. Li, Extracellular polymeric substances (EPS) of microbial aggregates in biological wastewater treatment systems: A review, Biotechnol. Adv. 28 (6) (2010) 882–894.
[19] Z. Teng, W. Shao, K. Zhang, Y. Huo, J. Zhu, M. Li, Pb biosorption by Leclercia adecarboxylata: Protective and immobilized mechanisms of extracellular polymeric substances, Chem. Eng. J. 375 (2019), 122113.
[20] W.-J. Ma, Z.-Q. Ren, L.-Q. Yu, X.-X. Wu, Y.-X. Yao, J.-T. Zhang, J.-Y. Guo, N.-S. Fan, R.-C. Jin, Deciphering the response of anammox process to heavy metal and antibiotic stress: Arsenic enhances the permeability of extracellular polymeric substance and aggravates the inhibition of sulfamethoxazole, Chem. Eng. J. 426 (2021), 130815.
[21] M. Zhang, Y. Peng, C. Wang, C. Wang, W. Zhao, W. Zeng, Optimization denitrifying phosphorus removal at different hydraulic retention times in a novel anaerobic anoxic oxic-biological contact oxidation process, Biochem. Eng. J. 106 (2016) 26–36.
[22] Z. Zhang, H. Xi, Y. Yu, Y. Zhou, Performance and prediction model of a HA+A/O process in the lab-scale under the load shock of 2,4-dichlorophenol, Process Saf. Environ. Prot. 130 (2019) 31–38.
[23] C. Wu, Y. Zhou, Q. Sun, L. Fu, H. Xi, Y. Yu, R. Yu, Appling hydrolysis acidification-anoxic–oxic process in the treatment of petrochemical wastewater: From bench scale reactor to full scale wastewater treatment plant, J. Hazard. Mater. 309 (2016) 185–191.
[24] F.-L. Sun, L.-L. Fan, Y.-S. Wang, L.-Y. Huang, Metagenomic analysis of the inhibitory effect of chromium on microbial communities and removal efficiency in A2O sludge, J. Hazard. Mater. 368 (2019) 523–529.
[25] K. Shi, H. Cheng, C.R. Cornell, H. Wu, S. Gao, J. Jiang, T. Liu, A. Wang, J. Zhou, B. Liang, Micro-aeration assisted with electrogenic respiration enhanced the microbial catabolism and ammonification of aromatic amines in industrial wastewater, J. Hazard. Mater. 448 (2023), 130943.
[26] G.-F. Li, W.-J. Ma, Z.-Q. Ren, Y.e. Wang, J.-P. Li, J.-W. Zhao, S.-T. Li, Q.i. Liu, Y.-N. Gu, Y.-F. Cheng, B.-C. Huang, R.-C. Jin, Molecular Insight into the Binding Property and Mechanism of Sulfamethoxazole to Extracellular Proteins of Anammox Sludge, Environ. Sci. Tech. 55 (24) (2021) 16627–16635.
[27] H. Wang, H. Yun, M. Li, H. Cui, X. Ma, Y. Zhang, X. Pei, L. Zhang, K. Shi, Z. Li, B. Liang, A. Wang, J. Zhou, Fate, toxicity and effect of triclocarban on the microbial community in wastewater treatment systems, J. Hazard. Mater. 440 (2022), 129796.
[28] Z.W. He, Z.S. Zou, Q. Sun, H.Y. Jin, X.Y. Yao, W.J. Yang, C.C. Tang, A.J. Zhou, W. Z. Liu, Y.X. Ren, A.J. Wang, Freezing-low temperature treatment facilitates short-chain fatty acids production from waste activated sludge with short-term fermentation, Bioresource Technol 347 (2022), 126337.
[29] M. DuBois, K.A. Gilles, J.K. Hamilton, P.A. Rebers, F. Smith, Colorimetric Method for Determination of Sugars and Related Substances, Anal. Chem. 28 (3) (1956) 350–356.
[30] Y. Bian, D. Wang, X. Liu, Q. Yang, Y. Liu, Q. Wang, B.J. Ni, H. Li, Y. Zhang, The fate and impact of TCC in nitrifying cultures, Water Res. 178 (2020), 115851.
[31] S. Wang, B. Ji, M. Zhang, Y. Ma, J. Gu, Y. Liu, Defensive responses of microalgal-bacterial granules to tetracycline in municipal wastewater treatment, Bioresource Technol 312 (2020), 123605.
[32] C. Kunacheva, D.C. Stuckey, Analytical methods for soluble microbial products (SMP) and extracellular polymers (ECP) in wastewater treatment systems: A review, Water Res. 61 (2014) 1–18.
[33] L. Miao, S. Wang, T. Cao, Y. Peng, M. Zhang, Z. Liu, Advanced nitrogen removal from landfill leachate via Anammox system based on Sequencing Biofilm Batch Reactor (SBBR): Effective protection of biofilm, Bioresource Technol 220 (2016) 8–16.
[34] W. Chen, P. Westerhoff, J.A. Leenheer, K. Booksh, Fluorescence Excitation−Emission Matrix Regional Integration to Quantify Spectra for Dissolved Organic Matter, Environ. Sci. Tech. 37 (24) (2003) 5701–5710.
[35] M.-H. Cui, L. Chen, Q. Zhang, L.-Y. Liu, H. Pan, H. Liu, A.-J. Wang, Understanding the effects of sludge characteristics on the biosorption of triclosan, Sci. Total Environ. 842 (2022), 156665.
[36] J. Xu, G.-P. Sheng, Y. Ma, L.-F. Wang, H.-Q. Yu, Roles of extracellular polymeric substances (EPS) in the migration and removal of sulfamethazine in activated sludge system, Water Res. 47 (14) (2013) 5298–5306.
[37] D. Wang, L. Tao, J. Yang, Z. Xu, Q. Yang, Y. Zhang, X. Liu, Q. Liu, J. Huang, Understanding the interaction between triclocarban and denitrifiers, J. Hazard. Mater. 401 (2021), 123343.
[38] X. Sheng, J. Wang, Q. Cui, W. Zhang, X. Zhu, A feasible biochar derived from biogas residue and its application in the efficient adsorption of tetracycline from an aqueous solution, Environ. Res. 207 (2022), 112175.
[39] A. Baker, Fluorescence Excitation−Emission Matrix Characterization of Some Sewage-Impacted Rivers, Environ. Sci. Tech. 35 (5) (2001) 948–953.
[40] Y.-J. Hu, Y.i. Liu, X.-H. Xiao, Investigation of the Interaction between Berberine and Human Serum Albumin, Biomacromolecules 10 (3) (2009) 517–521.
[41] D. Wei, B. Wang, H.H. Ngo, W. Guo, F. Han, X. Wang, B. Du, Q. Wei, Role of extracellular polymeric substances in biosorption of dye wastewater using aerobic granular sludge, Bioresource Technol 185 (2015) 14–20.
[42] A. Chergui, R. Kerbachi, G.-A. Junter, Biosorption of hexacyanoferrate(III) complex anion to dead biomass of the basidiomycete Pleurotus mutilus: Biosorbent characterization and batch experiments, Chem. Eng. J. 147 (2009) 150–160.
[43] F. Jia, Q. Yang, X. Liu, X. Li, B. Li, L. Zhang, Y. Peng, Stratification of Extracellular Polymeric Substances (EPS) for Aggregated Anammox Microorganisms, Environ. Sci. Tech. 51 (6) (2017) 3260–3268.
[44] Z. Wang, Y. Ma, J. Wei, X. Chen, L. Cao, W. Weng, Q. Li, H. Guo, J. Su, Effects of sintering temperature on surface morphology/microstructure, in vitro degradability, mineralization and osteoblast response to magnesium phosphate as biomedical material, Sci Rep-Uk 7 (2017) 823.
[45] J. Shen, G. Huang, C. An, X. Xin, C. Huang, S. Rosendahl, Removal of Tetrabromobisphenol A by adsorption on pinecone-derived activated charcoals: Synchrotron FTIR, kinetics and surface functionality analyses, Bioresource Technol 247 (2018) 812–820.
[46] S.-N. Yuen, S.-M. Choi, D.L. Phillips, C.-Y. Ma, Raman and FTIR spectroscopic study of carboxymethylated non-starch polysaccharides, Food Chem. 114 (3) (2009) 1091–1098.
[47] T. Pflüger, C.F. Hernández, P. Lewe, F. Frank, H. Mertens, D. Svergun, M. W. Baumstark, V.Y. Lunin, M.S.M. Jetten, S.L.A. Andrade, Signaling ammonium across membranes through an ammonium sensor histidine kinase, Nat. Commun. 9 (2018) 164.
[48] M.Y. Lobanov, N.S. Bogatyreva, O.V. Galzitskaya, Radius of gyration as an indicator of protein structure compactness, Mol. Biol. 42 (4) (2008) 623–628.
[49] X. Huang, X. Huang, L. Guo, L. He, D. Xiao, J. Zhan, A. Wang, R. Liang, Comparative Transcriptome Analysis Provides Insights into the Resistance in Pueraria [Pueraria lobata (Willd.) Ohwi] in Response to Pseudo-Rust Disease, Int. J. Mol. Sci. 23 (9) (2022) 5223.